Journal of Materials Chemistry A

ROYAL SOCIETY OF CHEMISTRY

COMMUNICATION

View Article Online
View Journal | View Issue

Cite this: *J. Mater. Chem. A*, 2024, **12**, 28711

Received 4th June 2024
Accepted 8th September 2024

DOI: 10.1039/d4ta03871a

rsc.li/materials-a

Revealing the disrupted Li/vacancy structure in Co, Mg, and Al co-doped ultra-high Ni-rich cathodes†

Hang Li, *[ab] Weibo Hua,[c] Alexander Missyul,[d] Thomas Bergfeldt,[b] Michael Knapp,[b] Helmut Ehrenberg,[b] Feng Pan *[a] and Sylvio Indris *[be]

Li atoms are believed to rearrange during Li insertion/removal in $LiNiO_2$ cathodes in lithium-ion batteries, forming certain Li/vacancy ordering structures. Substitution of Ni by dopants is considered to hinder such orderings, which is related to a quasi-solid-solution behavior in phase transitions and improved battery cyclability. Previous studies investigate the disruptions by theoretical calculations, however, direct experimental evidence is missing. Herein, the disturbed Li/vacancy structures are first observed based on the *ex situ* ^{6}Li nuclear magnetic resonance measurement.

The use of rechargeable lithium-ion batteries in electric vehicles (EVs) has promoted the transfer from traditional fossil fuels to green and clean electricity.[1–4] The lifetime and specific capacity of the electrode materials are strongly influenced by the structural evolution during charging and discharging.[5–7] Anisotropic strain and stress are inevitably induced, yielding crystal structure fatigue, such as the formation of cracks.[8–10] For the layered $LiNiO_2$ (LNO) cathode, the phase transition at high voltages leads to microcracking and is correlated with rapid electrochemical performance decay.[11–13] A doping strategy is often applied in LNO to obtain the commercialized cathode materials for EVs, *i.e.* Ni-rich cathode materials ($LiNi_xCo_yMn_{1-x-y}O_2$ or $LiNi_xCo_yAl_{1-x-y}O_2$).[14–18] The dopants are believed to introduce a quasi-solid-solution manner in phase transitions by disrupting the Li/vacancy orderings.[19–23] Although theoretical calculations have been performed to simulate such disruption,[19] the experimental findings of how dopants are located and disturb the Li ordering are still missing. Here the disturbed Li ordering structures are first revealed by analyzing the *ex situ* ^{6}Li nuclear magnetic resonance (NMR) spectra.

$LiNi_{0.94}Co_{0.03}Mg_{0.02}Al_{0.01}O_2$ (LNCMA) and $LiNiO_2$ (LNO) were synthesized by using a typical co-precipitation method followed by the annealing process (more information can be found in the ESI†). The inductively coupled plasma-optical emission spectroscopy (ICP-OES) proves that the dopants' atomic ratios are well-matched with the designed formulae (Table S1†). Statistical synchrotron-based powder X-ray diffraction (XRD) and refinements (Fig. S1, Tables S2 and S3†) confirm that LNCMA and LNO have a hexagonal α-$NaFeO_2$-type layered structure belonging to a space group of $R\bar{3}m$. The result of Rietveld refinement against XRD patterns shows a similar amount of Ni in Li layers (1.7% for LNCMA and 2.2% for LNO).[24] The z coordinate of oxygen (z/c) increases after doping, corresponding to the motion of O^{2-} closer to the Ni ions at (0 0 0). Such movement induces a decreasing bond length of Ni–O and an increasing bond length of Li–O. The valence state of Ni in LNCMA and LNO is studied by an X-ray absorption near-edge structure (XANES) experiment (Fig. S2†). The Ni K-edges of the two materials nearly overlap with each other, suggesting the oxidation states of Ni are predominantly +3. Fourier transform (FT) of the extended X-ray absorption fine structure (EXAFS) spectra (Fig. S3†) show that LNCMA has a slightly shorter Ni–O distance than LNO, in line with the decreased Ni–O bond length after doping. The decrease in Ni–O bond length is induced by the Mg^{2+}, which slightly increases the average Ni oxidation state for electroneutrality, leading to a motion of O^{2-} (ionic radius: Ni^{3+} ($r = 0.56$ Å), Ni^{4+}($r = 0.48$ Å)).

To investigate the phase transition behaviors of these two cathodes, dQ/dV (Q is the capacity and V is the voltage) profiles are plotted in Fig. 1 (the cells were tested at a rate of C/10 and 25 °C). Four peaks correspond to the kinetic hindrance peak in the H1 phase, the H1 to M, M to H2, and H2 to H3 phase transitions, respectively.[25–28] The peaks of LNCMA were greatly diminished when compared to those of LNO, indicating Li

[a]*School of Advanced Materials, Peking University, Shenzhen Graduate School, Shenzhen 518055, China. E-mail: 2206393335@pku.edu.cn; panfeng@pkusz.edu.cn*

[b]*Institute for Applied Materials (IAM), Karlsruhe Institute of Technology (KIT), Eggenstein-Leopoldshafen 76344, Baden-Württemberg, Germany. E-mail: sylvio.indris@kit.edu*

[c]*School of Chemical Engineering and Technology, Xi'an, Shanxi, 710049, China*

[d]*CELLS-ALBA, Synchrotron, Barcelona E-08290, Spain*

[e]*Applied Chemistry and Engineering Research Centre of Excellence (ACER CoE), Université Mohammed VI Polytechnique (UM6P), Lot 660, Hay Moulay Rachid, Ben Guerir, 43150, Morocco*

† Electronic supplementary information (ESI) available: See DOI: https://doi.org/10.1039/d4ta03871a

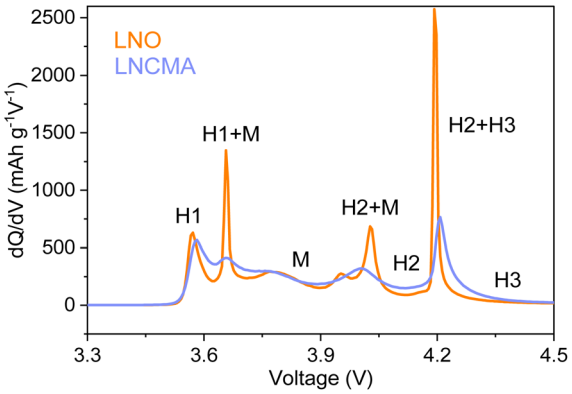

Fig. 1 The differential capacity (dQ/dV) curves of LNO and LNCMA.

removal occurs in a quasi-solid-solution rather than a pure two-phase reaction. Compared to electrochemical signals in dQ/dV curves, diffraction characterization offers more precise confirmation of phase transitions. *In situ* synchrotron XRD experiments were employed on LNCMA cathodes during the first charge period with a large voltage window of 2.8–4.7 V at a current density of 18 mA g^{-1} (The detailed voltage profiles are provided in Fig. S4†). The contour plots of 003 reflections of LNCMA and LNO are displayed in Fig. 2 (more reflections can be found in Fig. S5†). The phase transitions of LNO were discussed in detail in our recent paper.[29] For LNO, a new 003 reflection appears above 4.1 V at an angle that is 0.3° higher than that of the previous one. The co-existence of the two 003 reflections implies that in this period the Li removal occurs by a two-phase reaction, where the new Li-poor H3 phase nucleates and grows at the expense of the H2 phase.[30,31] In sharp contrast, introducing dopants induces a route change to a quasi-solid-solution manner, where only a single peak can be obtained during the whole charging process. The corresponding changes in lattice parameters are shown in (Fig. S6†). The suppressed phase transitions in LNCMA result in greatly improved capacity retention when compared with that of LNO and also of LNCO ($LiNi_{0.97}Co_{0.03}O_2$)(Fig. S7†). The Electrochemical impedance spectroscopy (EIS) was also performed during the cycling process (Fig. S8†).

Ex situ ^{6}Li solid-state NMR experiments were performed on LNCMA cathodes with different states of charge (SoC). A full comparison between the spectra of LNCMA and LNO is displayed in Fig. S9 (the pristine state) and S10.† The data of LNO was reported in our previous report where multiple Li/vacancy ordering structures of LNO were discussed in detail.[29] A detailed discussion about the special features of LNO spectra is provided in Note 1 (ESI†). As shown in Fig. 3, the two cathodes exhibit different behaviors at high SoC: there is an obvious increase in the NMR shift at SoC 75% for LNO and the peak position remains almost unchanged for the last three spectra (SoC 75–85%); in sharp contrast, the NMR signals keep moving to lower shift values for LNCMA from SoC 65% to Soc 85%. Such a difference indicates diverse Li local environments in these two cathodes on Li removal. For Ni-rich materials, the ^{6}Li chemical shifts are dominated by the Fermi contact interaction, which originates from the delocalization of unpaired electron spin density from Ni d orbitals to the Li nucleus *via* the bridging oxygen atoms.[32,33] The contribution from each adjacent paramagnetic Ni ion is additive to the overall NMR shifts and the magnitude is highly correlated to the angle of the TM–O–Li bond.[34] Based on earlier experimental studies on $LiNi_{0.3}Co_{0.7}O_2$, a 90° and 180° Ni–O–Li bond can induce chemical shifts of −15 and 110 ppm, respectively.[35,36] Diamagnetic ions, including Co^{3+}, Mg^{2+}, and Al^{3+}, are believed to induce much smaller shifts.

As displayed in Fig. 4a, two Li/vacancy structures ($Li_{0.5}NiO_2$ and $Li_{0.25}NiO_2$, corresponding to states of SoC 50% and SoC 75%) have been first predicted by theoretical calculations and later observed through NMR measurement.[29,37–39] The

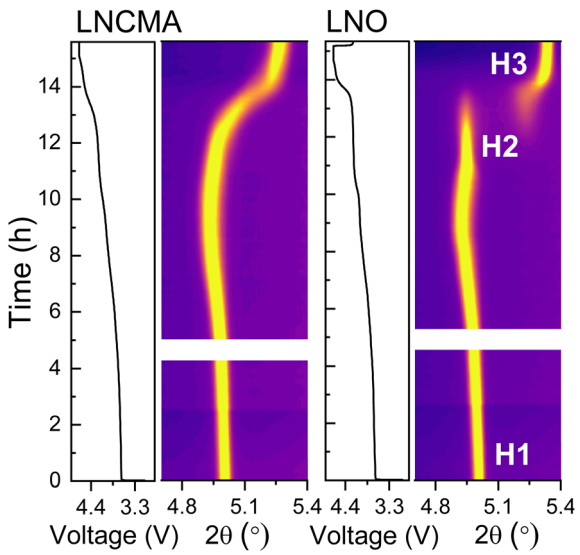

Fig. 2 The contour plot of the 003 reflection of the *in situ* XRD data (λ = 0.4130 Å). The left-hand subpanel shows the corresponding charge profiles.

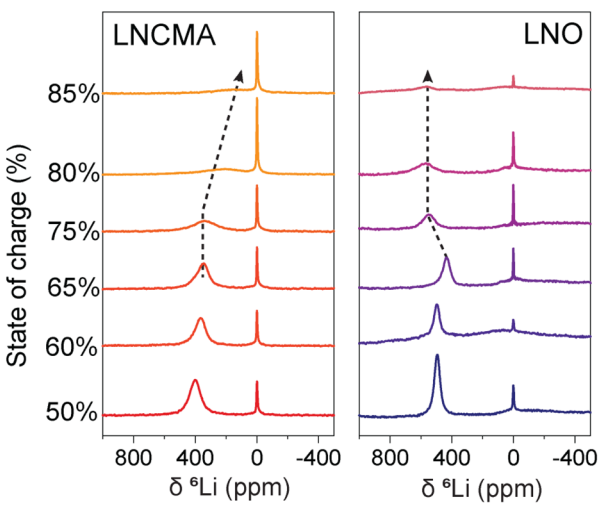

Fig. 3 Selected *ex situ* ^{6}Li solid-state NMR spectra of LNCMA and LNO cathodes with different SoCs.

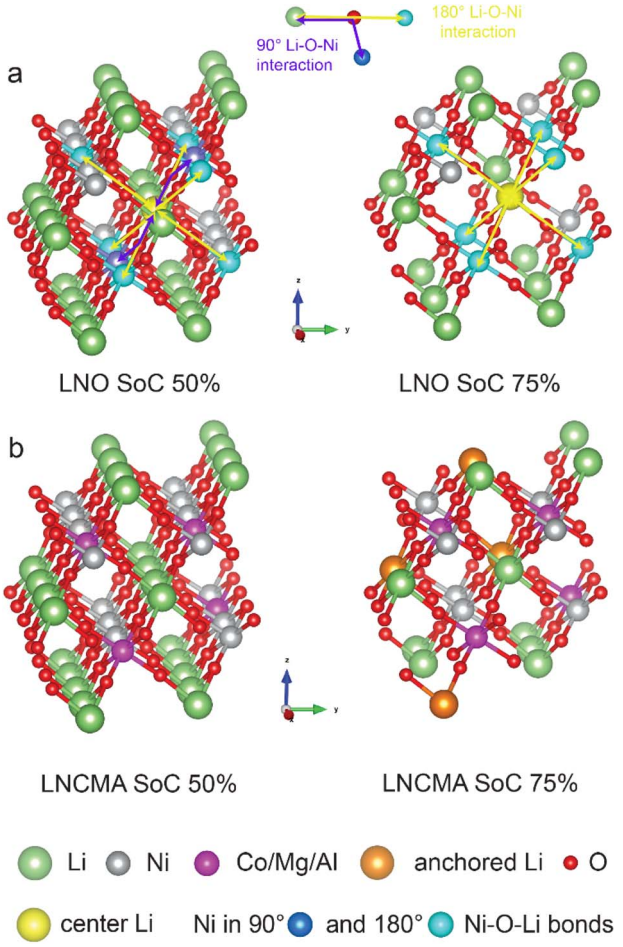

Fig. 4 Structural models of (a) LNO and (b) LNCMA cathodes at different SoCs.

simplified Li/vacancy distribution can be seen in Fig. 5. $Li_{0.5}NiO_2$ features alternating rows of full and vacant Li sites.[21,38] Each Li has six 180° and two 90° Ni–O–Li interactions and the predicted NMR shift is 630 ppm. Regarding $Li_{0.25}NiO_2$, it is formed by removing half of the Li in the full-filled Li rows in $Li_{0.5}NiO_2$. The remaining Li is separated by vacancies. Since the

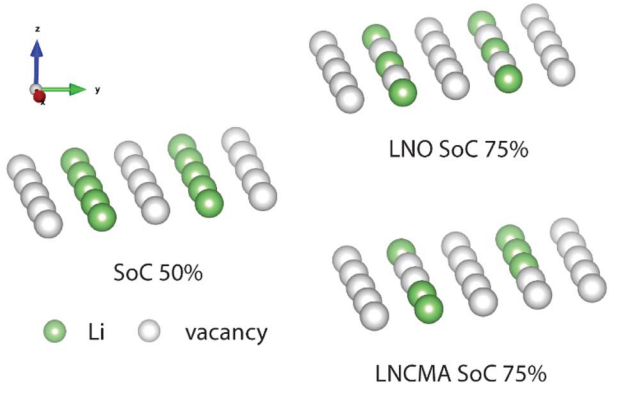

Fig. 5 A schematic image showing the Li arrangement in only one Li layer.

Li-vacancy ordering in the Li layer occurs concomitantly with a Ni^{3+}–Ni^{4+} ordering in the Ni layer,[29,39] each Li is surrounded by only six 180° Li–O–Ni^{3+} bonds, giving rise to a calculated shift of 660 ppm. The Li coordination situations are displayed in Fig. 4a, where the Li, Ni at 180° and 90° bonds are marked with yellow, light blue, and dark blue. When diamagnetic dopants are introduced into the LNO lattice, they are believed to be mainly placed at Ni rows in $Li_{0.5}NiO_2$ (Fig. 4b). The discussion on dopant occupation sites is provided in Note 2 (ESI†). Each Li is averagely coordinated by one 180° X–O–Li bond (X represents dopant), thus decreasing the original number of 180° Ni–O–Li interactions to five. The overall chemical shift then changes from 630 to 520 ppm for LNCMA at SoC 50%. Table 1 compares the experimental and calculated shifts for both LNO and LNCMA. The experimental shift is compatible with that calculated from the Li/vacancy models if the difference in bond length and bond angle between LNO and $LiNi_{0.3}Co_{0.7}O_2$ (where the reference values are obtained) is considered.[36,39] Note that the difference between experimental and predicted values is indeed similar for all three cases.

On further Li removal from LNCMA of SoC 50%, the structure still tries to form the same arrangement of Li and vacancies as in $Li_{0.25}NiO_2$, but that is impossible when Li at some specific sites is anchored by inactive dopants (Mg and Al).[20] That anchoring effect was proposed by J. R. Dahn through their first-principle calculations: Li atoms tend to be located in vertex-sharing sites relative to substituent sites of Mg and Al for the lowest energy; for Mg, two such Li atoms are located in the layers above and below Mg atoms and the number for Al is one; these Li atoms are proven to be inactive during Li deintercalation by the corresponding capacity penalty;[20] since Mg and Al are randomly distributed in the TM layers, nearby fixed inactive Li disturbs Li/vacancy orderings.

Note that Li in vertex-sharing sites just corresponds to the Li featuring a 180° Li–O–Mg(Al) configuration. As displayed in Fig. 4b, when half of the remaining Li is removed from the SoC 50% state of LNCMA, some Li atoms (labeled with orange color) are anchored by the neighboring Mg/Al dopants. Such Li atoms have one 180° Li–O–Mg(Al) bond (vertex-sharing). As a result, the original ordering scheme in $Li_{0.25}NiO_2$ is disrupted by these randomly distributed Li atoms (see Fig. 5). Some vacancies in $Li_{0.25}NiO_2$ orderings are occupied by the pinned Li atoms; some occupied Li sites are replaced with vacancies because these Li have to be deintercalated to provide capacity. The phase transitions in LNO are believed to be correlated to the Li/vacancy orderings.[40] The $Li_{0.25}NiO_2$ ordering corresponds to the structure of the H2 phase.[21] Upon further Li removal from LNO, the

Table 1 Comparison between the observed and estimated shifts for the NMR spectra

Name SoC%	Observed shifts (ppm)	Estimated shifts (ppm)	Difference (ppm)
LNO 50%	494	630	136
LNO 75%	548	660	112
LNCMA 50%	396	520	124

NMR peak stays at the same shift position with decreased intensity (see the NMR spectra of SoC 80% and 85%), indicating that the Li removal occurs through a two-phase reaction: Li is continuously deintercalated from the H2 phase to form the H3 phase. In contrast, the NMR signal of LNCMA keeps moving to lower ppm positions, suggesting a solid-solution manner, where Li is removed from the whole lattice. S. Sicolo *et al.* proposed that a disrupted Li ordering can suppress phase transitions by element substitution, as evidenced *via* Monte Carlo simulations at the Density Functional Theory level.[19] Our study verifies this calculation and provides a detailed scheme of how Li/vacancy orderings are disturbed. Note that defects of Ni in Li layers can also influence the Li/vacancy orderings, but this issue does not influence the comparison between LNO and LNCMA, owing to their similar values of Ni in Li layers. The thermal stability of charged electrodes is investigated by Synchrotron-based *in situ* heating XRD (Fig. S11†). Similar thermal behaviors are observed, indicating that a small number of dopants could not induce a comparatively profound effect on the thermal stability as their effect on the phase transition behavior.

Conclusions

In conclusion, the Li/vacancy structures including dopant occupation at highly charged states were described for Co, Mg, and Al co-doped cathodes. Based on those structures, the predicted chemical shifts are in line with the experimental ones, verifying the accuracy of the dopants' location. In the lattice, some Li atoms are anchored by the neighboring dopants, which disrupts the original Li/vacancy orderings. Such findings provide direct experimental support to previous assumptions for the first time and pave the way for further research.

Data availability

The authors confirm that the data supporting the findings of this study are available within the article and its ESI.†

Author contributions

Feng Pan, Helmut Ehrenberg, and Sylvio Indris directed the research projects and supervised the work. Hang Li conducted the experiments, summarized the data, and wrote the original draft. Weibo Hua, Alexander Missyul, and Thomas Bergfeldt provide help in the characterization. All authors discussed the results and contributed to the paper.

Conflicts of interest

There are no conflicts to declare.

Acknowledgements

This work is supported by the China and Germany Postdoctoral Exchange Program (HGF-OCPC) between Peking University and Karlsruhe Institute of Technology (KIT) under program no. ZD2022028, the Basic and Applied Basic Research Foundation of Guangdong Province (no. 2021B1515130002), the Soft Science Research Project of Guangdong Province (no. 2017B030301013), and the Shenzhen Science and Technology Research Grant (no. ZDSYS201707281026184). The research used the resources of the P65 beamline of the PETRA III at DESY (Hamburg, Germany), a member of the Helmholtz Association. This research used resources from the MS beamline of Paul Scherrer Institute (PSI), Villigen, Switzerland. Beamline scientist is Nicola Pietro Maria Casati. This research used resources of the MSPD beamline at the ALBA synchrotron (Barcelona, Spain) under proposal no. 2020024304-hli. This work contributes to the research performed at CELEST (Center for Electrochemical Energy Storage Ulm-Karlsruhe).

Notes and references

1 R. Schmuch, R. Wagner, G. Hörpel, T. Placke and M. Winter, *Nat. Energy*, 2018, **3**, 267.
2 A. Manthiram and J. B. Goodenough, *Nat. Energy*, 2021, **6**, 323.
3 G.-T. Park, B. Namkoong, S.-B. Kim, J. Liu, C. S. Yoon and Y.-K. Sun, *Nat. Energy*, 2022, **7**, 946.
4 L. Wang, T. Liu, T. Wu and J. Lu, *Nature*, 2022, **611**, 61.
5 B. Li, G. Rousse, L. Zhang, M. Avdeev, M. Deschamps, A. M. Abakumov and J. M. Tarascon, *Energy Environ. Sci.*, 2023, **16**, 1210.
6 D. Luo, H. Zhu, Y. Xia, Z. Yin, Y. Qin, T. Li, Q. Zhang, L. Gu, Y. Peng, J. Zhang, K. M. Wiaderek, Y. Huang, T. Yang, Y. Tang, S. Lan, Y. Ren, W. Lu, C. M. Wolverton and Q. Liu, *Nat. Energy*, 2023, **8**, 1078.
7 R. Zhang, C. Wang, P. Zou, R. Lin, L. Ma, L. Yin, T. Li, W. Xu, H. Jia, Q. Li, S. Sainio, K. Kisslinger, S. E. Trask, S. N. Ehrlich, Y. Yang, A. M. Kiss, M. Ge, B. J. Polzin, S. J. Lee, W. Xu, Y. Ren and H. L. Xin, *Nature*, 2022, **610**, 67.
8 H. Zhu, Z. Wang, L. Chen, Y. Hu, H. Jiang and C. Li, *Adv. Mater.*, 2023, **35**, 2209357.
9 H. Li, A. Liu, N. Zhang, Y. Wang, S. Yin, H. Wu and J. R. Dahn, *Chem. Mater.*, 2019, **31**, 7574.
10 H. H. Ryu, K. J. Park, C. S. Yoon and Y. K. Sun, *Chem. Mater.*, 2018, **30**, 1155.
11 C. S. Yoon, D. W. Jun, S. T. Myung and Y. K. Sun, *ACS Energy Lett.*, 2017, **2**, 1150.
12 G. W. Nam, N. Y. Park, K. J. Park, J. Yang, J. Liu, C. S. Yoon and Y. K. Sun, *ACS Energy Lett.*, 2019, **4**, 2995.
13 H. J. Noh, S. Youn, C. S. Yoon and Y. K. Sun, *J. Power Sources*, 2013, **233**, 121.
14 W. Liu, P. Oh, X. Liu, M. J. Lee, W. Cho, S. Chae, Y. Kim and J. Cho, *Angew. Chem., Int. Ed.*, 2015, **54**, 4440.
15 M. Bianchini, M. Roca-Ayats, P. Hartmann, T. Brezesinski and J. Janek, *Angew. Chem., Int. Ed.*, 2019, **58**, 10434.
16 W. Hua, J. Zhang, S. Wang, Y. Cheng, H. Li, J. Tseng, Z. Wu, C. H. Shen, O. Dolotko, H. Liu, S. F. Hung, W. Tang, M. Li, M. Knapp, H. Ehrenberg, S. Indris and X. Guo, *Angew. Chem., Int. Ed.*, 2023, **62**, e20221488.

17 A. Grenier, P. J. Reeves, H. Liu, I. D. Seymour, K. Märker, K. M. Wiaderek, P. J. Chupas, C. P. Grey and K. W. Chapman, *J. Am. Chem. Soc.*, 2020, **142**, 7001.
18 H. Li, P. Zhou, F. Liu, H. Li, F. Cheng and J. Chen, *Chem. Sci.*, 2019, **10**, 1374.
19 M. Mock, M. Bianchini, F. Fauth, K. Albe and S. Sicolo, *J. Mater. Chem. A*, 2021, **9**, 14928.
20 H. Li, M. Cormier, N. Zhang, J. Inglis, J. Li and J. R. Dahn, *J. Electrochem. Soc.*, 2019, **166**, A429.
21 M. E. Arroyo y de Dompablo and G. Ceder, *J. Power Sources*, 2003, **119–121**, 654.
22 M. E. Arroyo y de Dompablo, A. Van der Ven and G. Ceder, *Phys. Rev. B: Condens. Matter Mater. Phys.*, 2002, **66**, 1.
23 H. Das, A. Urban, W. Huang and G. Ceder, *Chem. Mater.*, 2017, **29**, 7840.
24 D. Goonetilleke, B. Schwarz, H. Li, F. Fauth, E. Suard, S. Mangold, S. Indris, T. Brezesinski, M. Bianchini and D. Weber, *J. Mater. Chem. A*, 2023, **11**, 13468.
25 H. Li, N. Zhang, J. Li and J. R. Dahn, *J. Electrochem. Soc.*, 2018, **165**, A2985.
26 L. de Biasi, A. Schiele, M. Roca-Ayats, G. Garcia, T. Brezesinski, P. Hartmann and J. Janek, *ChemSusChem*, 2019, **12**, 2240.
27 A. Hirano, R. Kanno, Y. Kawamoto, Y. Takeda, K. Yamaura, M. Takano, K. Ohyama, M. Ohashi and Y. Yamaguchi, *Solid State Ionics*, 1995, **78**, 123.
28 T. Ohzuku, A. Ueda and M. Nagayama, *J. Electrochem. Soc.*, 1993, **140**, 1862.
29 H. Li, W. Hua, X. Liu-Théato, Q. Fu, M. Desmau, A. Missyul, M. Knapp, H. Ehrenberg and S. Indris, *Chem. Mater.*, 2021, **33**, 9546.
30 W. Li, J. N. Reimers and J. R. Dahn, *Solid State Ionics*, 1993, **67**, 123.
31 M. Z. Bazant, *Acc. Chem. Res.*, 2013, **46**, 1144.
32 C. Delmas, D. Carlier, G. Ceder, M. Ménétrier and C. P. Grey, *Phys. Rev. B: Condens. Matter Mater. Phys.*, 2003, **67**, 174103.
33 C. P. Grey and N. Dupré, *Chem. Rev.*, 2004, **104**, 4493.
34 K. Märker, P. J. Reeves, C. Xu, K. J. Griffith and C. P. Grey, *Chem. Mater.*, 2019, **31**, 2545.
35 D. Zeng, J. Cabana, J. Bréger, W. S. Yoon and C. P. Grey, *Chem. Mater.*, 2007, **19**, 6277.
36 D. Carlier, M. Ménétrier and C. Delmas, *J. Mater. Chem.*, 2001, **11**, 594.
37 Y. Takahashi, N. Kijima, K. Tokiwa, T. Watanabe and J. Akimoto, *J. Phys.: Condens.Matter*, 2007, **19**, 436202.
38 J. P. Peres, F. Weill and C. Delmas, *Solid State Ionics*, 1999, **116**, 19.
39 C. Chazel, M. Ménétrier, L. Croguennec and C. Delmas, *Inorg. Chem.*, 2006, **45**, 1184.
40 C. Xu, P. J. Reeves, Q. Jacquet and C. P. Grey, *Adv. Energy Mater.*, 2021, **11**, 2003404.